Spring 5-5-2011

Critical Evaluation of Euler-Euler and Euler-Lagrangian Modelling Strategies in a 2-D Gas Fluidized Bed

F. Hernández-Jiménez
Carlos III University of Madrid, Spain

J. R. Third
ETH Zürich, Switzerland

A. Acosta-Iborra
Carlos III University of Madrid, Spain

C. R, Müller
ETH Zürich, Switzerland

CRITICAL EVALUATION OF EULER-EULER AND EULER-LAGRANGIAN MODELLING STRATEGIES IN A 2-D GAS FLUIDIZED BED

F. Hernández-Jiménez[a], J.R. Third[b], A. Acosta-Iborra[a], C.R. Müller[b]

[a]Universidad Carlos III of Madrid, Department of Thermal and Fluid Engineering, ISE research group. Av. de la Universidad, 30, 28911, Leganés, Madrid, Spain .

[b]ETH Zürich, Institute of Energy Technology, Laboratory of Energy Science and Engineering, Leonhardstrasse 27, 8092 Zürich, Switzerland.

Abstract

Two-phase granular systems are commonly encountered in industry, and fluidized beds are particularly important due to their excellent heat and mass transfer characteristics. Here, we critically evaluate the differences between two modelling strategies, Euler-Euler and Euler-Lagrangian models. Euler-Euler simulations were performed using MFIX and an in-house code was used for Euler-Lagrangian simulations. A 2D bed of width, height and transverse thickness of respectively, 0.2 m, 0.5 m and 0.01 m, served as a test case. The settled bed height was H_0 = 0.2 m. Particles of density ρ = 1000 kg/m³ and diameter d_p = 1.2 mm were fluidized with air. The drag-law proposed by Benyahia *et al.* (10) was used in both models. Comparison between the simulation results was based on both instantaneous and time-averaged properties. A particular focus of this study was the influence of the coefficients of restitution and friction on the simulation results.

INTRODUCTION

Fluidized beds have various applications in industry, such as fluid catalytic cracking (FCC), gasification and combustion of coal, and Fischer−Tropsch synthesis (Kunii and Levenspiel (1)). Despite the fact that fluidized beds have been used in industry since the 1920s and good progress has been made in numerical simulations using two-fluid (Gidaspow (2)) or discrete element models (Tsuji et al. (3)), some aspects of fluidized bed hydrodynamics, such as bubble splitting, are still far from fully understood.

Numerical modelling of fluidized beds has advanced significantly over the last two decades, the most popular modelling approaches being the Euler-Euler and Euler-Lagrangian models. The Euler-Lagrangian approach combines an Eulerian description of the fluid-phase with a Lagrangian particle simulation, in which the trajectory of each particle is calculated based on Newton's second Law. The gas-solids interaction is computed through semi-empirical closure models (Deen et al. (4)). Although very promising, the Euler-Lagrangian approach is very computationally expensive and is, therefore, currently unable to simulate the large number of particles encountered in medium- or large-scale fluidized beds. In the Euler-Euler approach (Gidaspow (2), Wachem and Almstedt (5)) the particulates and the fluid phase are treated as inter-penetrating continua (two-fluid model). As in

the case of the Euler-Lagrangian approach, two-fluid simulations of fluidized beds require closure relationships for the gas-solids interaction. However, since the particle motion is not modelled in detail, the two-fluid model also requires closure relationships for the particle-particle interactions. These closure relationships may be empirical in nature or may be derived from theoretical relations that are linked to the kinetic theory of granular gases (Gidaspow (2)).

The aim of this work is to compare the Euler-Euler and Euler-Lagrangian approaches for a specific test case, consisting of a two-dimensional (2D) gas fluidized bed. In addition, the effect of parameters such as the inter-particle and particle-wall coefficients of friction, and the coefficient of restitution, will be studied for both models.

DEM APPROACH

A Discrete Element Model (DEM) has been constructed based on the work of Tsuji et al (3), which combines the discrete element model of Cundall and Strack (6) to simulate the particulate phase, with the volume-averaged Navier-Stokes equations for the fluid phase, as derived by Anderson and Jackson (7). For each particle, the linear and angular momenta are governed by Newton's second law:

$$m_p \frac{d\vec{v}_s}{dt} = -V_p \nabla p + \frac{V_p \beta}{(1-\alpha_g)}(\vec{v}_g - \vec{v}_s) + \vec{F}_c \qquad I_p \frac{d\vec{\omega}_s}{dt} = \vec{T}_p$$

where $m_p, \vec{v}_s, \vec{\omega}_s, V_p, \vec{v}_g, \beta, \vec{F}_c, \vec{T}_p$ and I_p are the mass, linear and angular velocities of the particle, the particle volume, the velocity of the gas phase, the inter-phase momentum exchange coefficient, the force and torque resulting from the collision of the particles, and the moment of inertia of the particle, respectively. To model the collision between contacting particles the soft-sphere approach was used, in which the particles are allowed to overlap by a small amount, δ. For the fluid the volume-averaged continuity and Navier-Stokes equations are given by Anderson and Jackson (7):

$$\frac{\partial \alpha_g \rho_g}{\partial t} + \nabla \cdot (\alpha_g \rho_g \vec{v}_g) = 0$$

$$\frac{\partial \alpha_g \rho_g \vec{v}_g}{\partial t} + \nabla \cdot (\alpha_g \rho_g \vec{v}_g{}^2) = -\alpha_g \nabla p - \nabla \cdot (\alpha_g \overline{\overline{\tau}}_g) - \vec{F}_p + \alpha_g \rho_g \vec{g}$$

here, $\overline{\overline{\tau}}_g$ is the viscous stress tensor and $\vec{F}_p$ is the rate of exchange of momentum between the particulate and the fluid phases. The fluid was assumed to be Newtonian. The rate of momentum exchange between the particulate and fluid phases was calculated by adding up the fluid forces acting on the N_p individual particles in a fluid cell of volume V_{cell} :

$$\vec{F}_p = \frac{V_p}{V_{cell}} \frac{\sum_{n=1}^{N_p} \beta(\vec{v}_g - \vec{v}_s)}{(1-\alpha_g)}$$

TWO-FLUID MODEL APPROACH

The two-fluid model, based on the conservation equations of mass, momentum and granular temperature, was solved using the MFIX code (Multifluid Flow with Interphase eXchanges) (Syamlal et al (8), Benyahia et al (9)). The kinetic theory of

granular gases was used for the closure of the solids pressure stress terms. The governing equations can be summarized as follows.

Mass conservation of the gas (g) and solid (s) phases:

$$\frac{\partial \alpha_g \rho_g}{\partial t} + \nabla \cdot (\alpha_g \rho_g \vec{v}_g) = 0 \qquad \frac{\partial \alpha_s \rho_s}{\partial t} + \nabla \cdot (\alpha_s \rho_s \vec{v}_s) = 0$$

Momentum conservation of the gas and solids phases:

$$\frac{\partial \alpha_g \rho_g \vec{v}_g}{\partial t} + \nabla \cdot (\alpha_g \rho_g \vec{v}_g) = -\alpha_g \nabla p + \nabla \cdot \overline{\overline{\tau}}_g + \alpha_g \rho_g \vec{g} - K_{gs}(\vec{v}_g - \vec{v}_s)$$

$$\frac{\partial \alpha_g \rho_g \vec{v}_g}{\partial t} + \nabla \cdot (\alpha_s \rho_s \vec{v}_s) = -\alpha_s \nabla p - \nabla p_s + \nabla \cdot \overline{\overline{\tau}}_s + \alpha_s \rho_s \vec{g} + K_{gs}(\vec{v}_g - \vec{v}_s)$$

where $\alpha_g, \alpha_s, \rho_g, \rho_s, \vec{v}_g, \vec{v}_g$ correspond to gas and solids volume fraction, gas and solids density and gas and solids velocity respectively, p is pressure, $\overline{\overline{\tau}}_g, \overline{\overline{\tau}}_s$ the stress tensors for gas and solids respectively, $\vec{g}$ is the acceleration due to the gravity and K_{gs} is the gas-solids momentum exchange coefficient.

The balance equation for the granular temperature, Θ, is given by:

$$\frac{3}{2}\left(\frac{\partial}{\partial t}(\alpha_s \rho_s \Theta) + \nabla \cdot (\alpha_s \rho_s \vec{v}_s \Theta)\right) = (-p_s \overline{\overline{I}} + \overline{\overline{\tau}}_s) : \nabla \vec{v}_s + \nabla \cdot (k_\Theta \nabla \Theta) - \gamma_\Theta - 3K_{gs}\Theta$$

where $-p_s \overline{\overline{I}} + \overline{\overline{\tau}}_s : \nabla \vec{v}_s$ is the generation of Θ by the solids stress tensor, $\nabla \cdot (k_\Theta \nabla \Theta)$ is the diffusion of Θ energy, γ_Θ is the collisional dissipation of energy and $3K_{gs}\Theta$ is the transfer of kinetic energy between phases. A second order accurate scheme (Superbee) was used to discretize the convective derivatives in the balance equations.

NUMERICAL SIMULATIONS

The gas-fluidized bed studied was of 0.2 m width, 0.01 m transverse thickness and 0.5 m height, filled with spherical particles of density ρ = 1000 kg/m³ and diameter d_p = 1.2 mm. The static bed height was H_0 = 0.2 m and the gas inlet velocity was U = 0.6 m/s, corresponding to U/U_{mf} = 2 . Several cases were studied to evaluate the effect of the properties of the particles and walls. Table 1 summarizes the cases studied in this work. The parameters that are varied are the inter-particle and particle-wall coefficients of friction, and the restitution coefficient. Case 1 is taken to be the base case incorporating commonly used parameters. The inlet has been modelled as a homogeneous velocity inlet and the outlet as a constant pressure outlet for both models. The computational domain for the two-fluid model simulations comprised 57 × 141 × 8 cells in the x- (width), y- (height) and z- (thickness) directions, respectively. This creates a mesh with a 3.5 mm cell size, which is below 10 particle diameters and ensures grid-independent results. A partial slip boundary condition was applied at the walls of the fluidized bed, with a partial slip coefficient of Φ=0.6. The fluid computational domain for the DEM model comprised 58 × 148 × 3 cells in the x-, y- and z- directions. The fluidized bed contained 265650 particles. Interactions between particles are modelled using a damped Hertzian spring with an E-modulus of 1.2×106 N/m2. Both models use the drag law proposed by Benyahia et al. (10). For the time-averaged results, 40 seconds are employed for the Euler-Euler model and 28 seconds for the Euler-Lagrangian model.

Model	Parameter	Case 1	Case 2	Case 3	Case 4
Two-fluid model	Restitution coefficient	0.9	0.9	0.9	0.5
	Coefficient of friction between particles	0.57	0.1	0.57	0.57
	Walls boundary conditions	Partial slip	Partial slip	Free slip	Partial slip
DEM	Restitution coefficient	0.9	0.9	0.9	0.5
	Coefficient of friction between particles	0.57	0.1	0.57	0.57
	Friction between particles and walls	0.57	0.1	0	0.57

Table 1: Simulation parameters for the two-fluid and DEM simulations.

RESULTS DISCUSSION

Figure 1 shows instantaneous snapshots of the solids volume fraction for case 1 simulated using the two models. Both snapshots were taken after the transient fluidization that occurs during start-up. The snapshots show the characteristic pattern of 2-D beds: small and narrow bubbles appearing in the bottom of the bed, and bigger and less numerous circular bubbles reaching the bed surface. Here bubbles are located where the solids volume fraction reaches a value close to zero. The solids volume fractions presented have been averaged over the entire bed thickness.

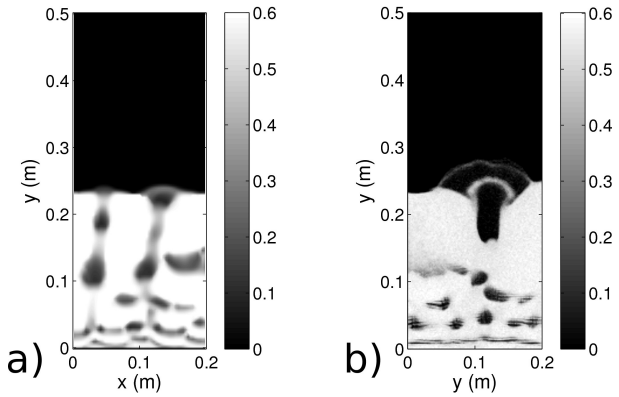

Figure 1. Instantaneous snapshot of the bed showing α_s: a) two-fluid model; b) DEM.

Figures 2 and 3 show the solids volume fraction averaged over the width and thickness of the bed, as a function of time, for the two fluid model and DEM respectively. Both models show the creation of small, slow-moving bubbles close to the distributor and the coalescence and eruption of faster bubbles at distances around y = 0.1 m above the distributor.

Figure 4a and 4b show the power spectra obtained from the data presented in Figures 2 and 3 at two different heights, y = 0.005 m (close the distributor) and y = 0.217 m (close to the top of the bed). For both models the maxima in the power spectra occur at higher frequencies at *y* = 0.005 m than at y = 0.217 m. This is expected because bubbles coalesce as they rise through the bed, leading to a reduction in the number of bubbles that cross a horizontal section.

It should be noted, however, that the frequency depicted in Figure 4 is a 'bubble coherence frequency' because several bubbles may cross a horizontal section at any instant of time. Therefore, the frequencies of Figure 4 cannot be interpreted as a single bubble frequency unless the size of the bubble is comparable to the bed width, i.e. near the bed surface. The bubble coherence frequency near the distributor defines the principal frequency of bubble formation. This frequency of bubble formation is qualitatively similar in both models, namely ~ 6 Hz. The principal frequencies at y = 0.217 m, i.e. the frequency of bubble eruption, are also similar for both simulation strategies. In particular, Figure 4 shows that the peak of the power spectrum at y = 0.217 m occurs at ~ 2.5 Hz, which is in agreement with the bed oscillation frequency due to bubble eruption given by Baskakov et al. (11), $f = \sqrt{g/H_o}/\pi = 2.23\,Hz$.

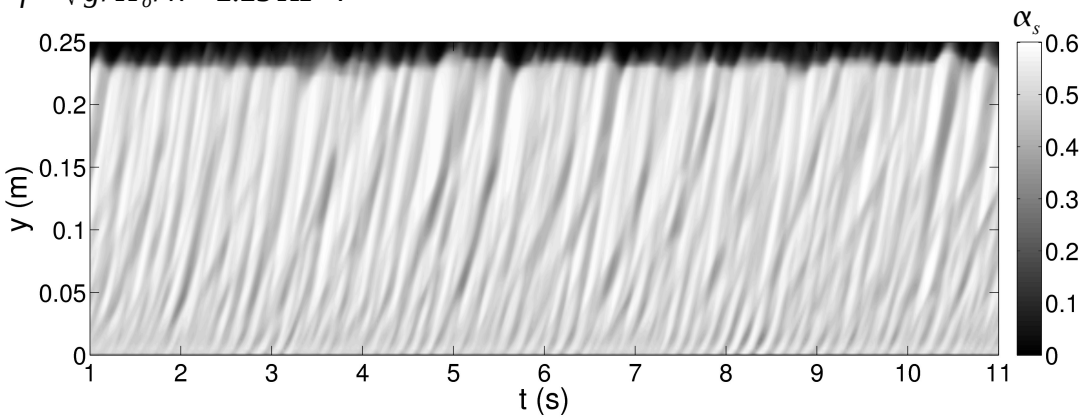

Figure 2. XZ-averaged α_s, two-fluid model. Case 1.

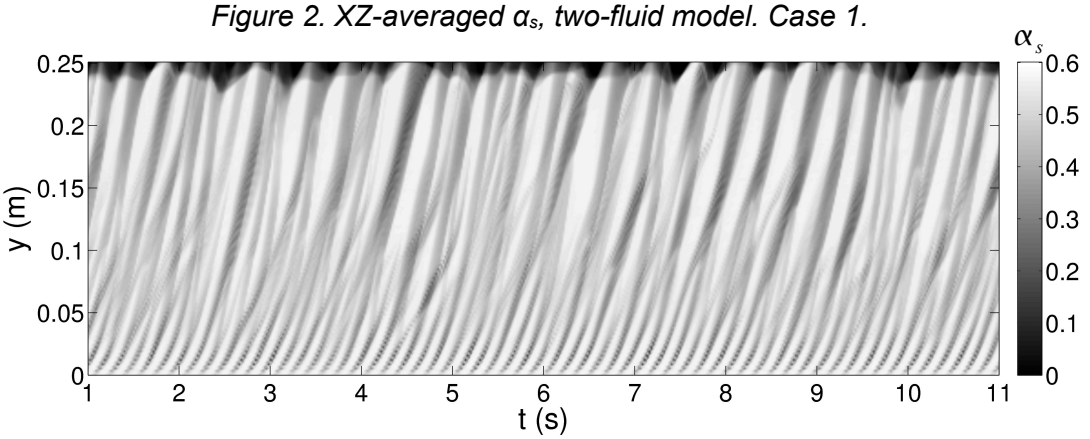

Figure 3. XZ-averaged α_s, DEM. Case 1.

The average solids volume fraction in an *x-z* plane located at *y* = 0.22 m is shown in Figure 5 for the two fluid model and DEM. This *y* position is close to the freeboard of the bed. Figure 5a reveals that the amplitude of the fluctuations in the solids volume fraction is smaller in the two-fluid simulations when compared with the DEM results. This is expected since the two-fluid approach tends to smear the distinction between the bubble and particulate phase. For the DEM a sharper, and more realistic, transition between the bubble and particulate phase is modeled.

Figure 5b plots the dominant frequencies, extracted as the peak-frequency from the power spectra, as a function of vertical position, *y*. In both simulation strategies, the

profiles of peak-frequencies are in good agreement. In particular, high frequencies (around 6 Hz) are observed near the distributor and there is a transition zone in 0.05 m < y < 0.1 m. Near the freeboard both simulations show a region where the frequency stabilizes due to big bubbles passing at a frequency around 2.5Hz. Figures 2 and 3 reinforce this observation: both figures indicate a large number of slow-moving bubbles close to the distributor and a smaller number of faster bubbles after the transition zone.

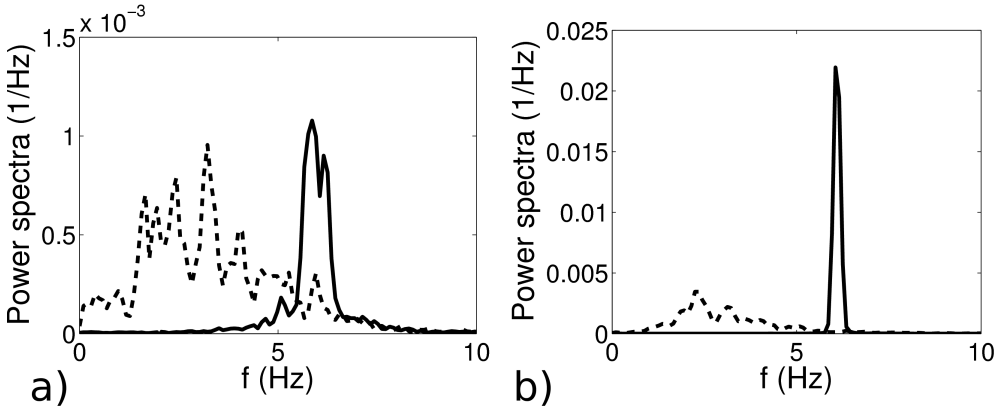

Figure 4. Power spectra of XZ-averaged α_s, a) two-fluid model, b) DEM. y = 0.005 m (solid line); y = 0.217 m (dash line). Case 1.

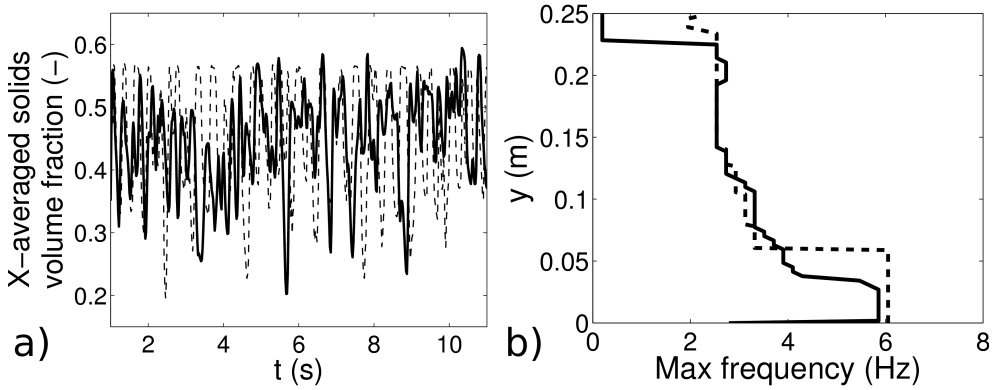

Figure 5. a) XZ-averaged α_s at a height of 0.22 m b) Vertical profile of peak frequency for XZ-averaged α_s: two-fluid model (solid line); DEM (dash line). Case 1.

The effect of the wall friction is demonstrated in Figures 6a and 6b. Here, the solids velocity and solids volume fraction, averaged with respect to time and transversal thickness, are presented at a height y = 0.01 m for both simulation strategies. In case 1, both models predict very similar magnitudes for the solids velocity, however the bed hydrodynamics are substantially different. In the two-fluid model there are two preferential bubble paths at a distance of ~ 0.05 m away from the lateral walls (Figure 6b). On the other hand in the DEM there is only one path in the middle of the bed. For case 3, which employs a free slip condition at the walls, the time-averaged velocities within the bed are an order of magnitude greater than those obtained for case 1. Furthermore, there are substantial discrepancies between the two-fluid and DEM results obtained for case 3: the two-fluid model predicts velocities that are approximately twice those predicted by the DEM and also predicts higher solids volume fractions, i.e. smaller bed expansion.

Finally, Figure 7 compares the solids velocity in both models for cases 1, 2 and 4. For the two-fluid model only small changes in the profile of the solids velocity can be observed for the case that the coefficients of friction and restitution are reduced. However, for the DEM the coefficient of friction plays an important role. Reducing the coefficient of friction in the DEM from 0.57 to 0.1 leads to a substantial increase in the time-averaged solids velocities, as seen in Figure 7b. Furthermore, it is observed that for the two-fluid model reducing the coefficient of restitution decreases the gradient along x-direction in the solids velocity profile; only very small variations were observed in the DEM results.

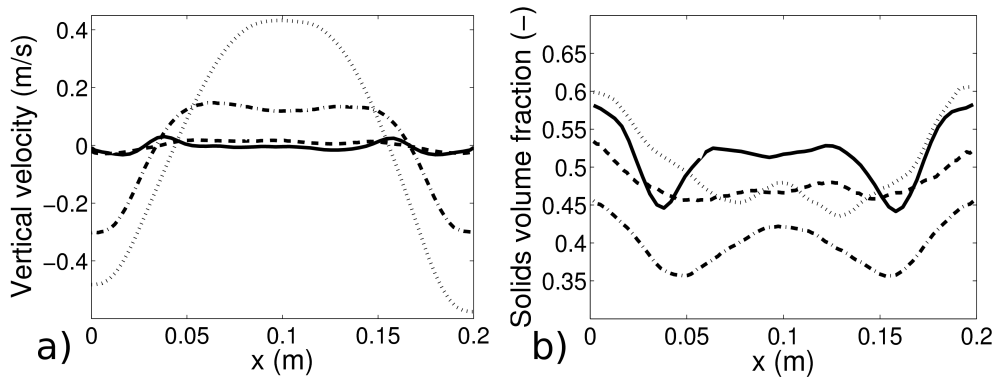

Figure 6. Time averaged values of a) solids vertical velocity and b) α_s at a height of 0.1 m: two-fluid model case 1 (solid line); DEM case 1 (dash line); two-fluid model case 3 (dot line); DEM case 3 (dash-dot line).

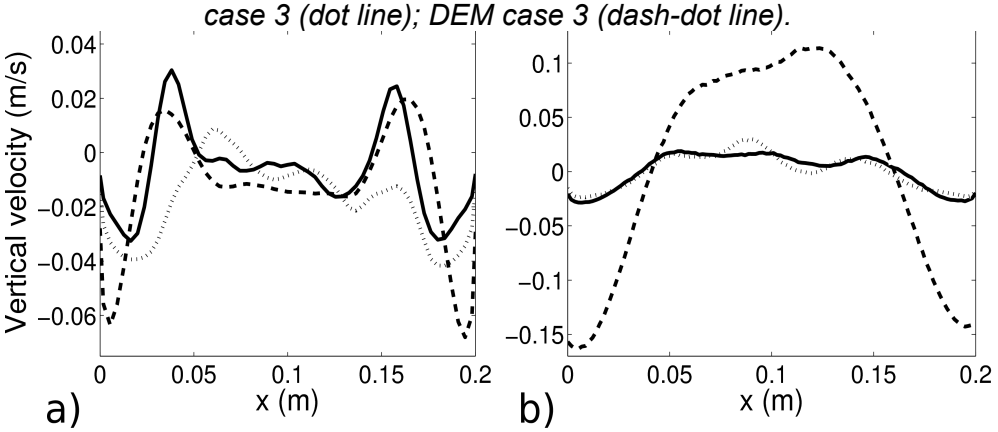

Figure 7. Time averaged values of solids vertical velocity at a height of 0.1 m, a) two-fluid model b) DEM: case 1 (solid line); case 2 (dash line); case 4 (dot line).

CONCLUSIONS

DEM and two-fluid model simulations of 2D bubbling fluidized beds have been compared in this work. For the base case, in which the coefficient of friction was set to 0.57, both simulation strategies yield time-averaged velocities with similar magnitudes, however the agreement of the characteristics of the velocity profiles is disappointing, especially for the case using zero friction for the particle-wall contact. The two-fluid model predicts that the highest velocities within the bed are located at a distance of ~ 0.05 m away from the side wall, whereas the DEM predicts that the highest velocities are located at the centre of the bed. For both simulation techniques, the time-averaged solids volume fractions show minima that are coincident with the maxima in the velocity profiles. This is consistent with the

hypothesis that bubbles preferentially pass through these locations.

The behaviour of bubbles has been examined by averaging the solids volume fraction over horizontal cross sections of the bed. Both the two-fluid and DEM simulations predict a coherence bubble frequency of 6 Hz close to the distributor and a frequency of 2.5 Hz close to the surface of the bed.

Furthermore, the influence of the coefficients of friction and restitution on the simulation results has been investigated. The time-averaged solids velocity and solids volume fraction profiles suggest that, within the range examined here, the behaviour of the bed, using two-fluid and DEM models, is relatively insensitive to the particle-particle coefficient of friction and, for the DEM results, to the coefficient of restitution. However, setting the particle-wall coefficient of friction to zero was found to have a pronounced effect on the particle motion within the bed. Under these conditions both models were found to give time-averaged solids velocities an order of magnitude larger than those predicted for simulations with particle-wall friction. Nevertheless, further work is required to establish the causes of the discrepancies between the DEM and two-fluid models highlighted here.

Acknowledgement

This work has been co-funded by the Spanish Government (Project DPI2009 -10518) and the Autonomous Community of Madrid (Project S2009/ENE-1660).

References

1. D. Kunii, O. Levenspiel, Fluidization Engineering: Butterworth-Heinemann: Newton, MA, 1991.
2. D. Gidaspow, Multiphase flow and Fluidization: Continuum and kinetic theory descriptions; Academic Press: San Diego, CA. 1994.
3. Y. Tsuji, T. Kawaguchi, T. Yanaka, Discrete particle simulations of 2-dimensional fluidized-beds. Powder tech. 77 (1993) 79-87.
4. N.G. Deen M. van Sint Annaland, M.A. van der Hoef, J.A.M. Kuipers, Review of discrete particle modelling of fluidized beds. Chem. Eng. Sci. 62 (2007) 28-44.
5. B.G.M. van Wachem, A.E. Almstedt, Methods for multiphase computational fluid dynamics. Chem. Eng J. 96 (2003) 81-98.
6. P.A. Cundall, C.D.L. Strack, A discrete numerical-model for granular assemblies. Geotechnique 29 (1979) 47-65.
7. T.B Anderson, R. Jackson, A fluid mechanical description of fluidized beds. Ind. Eng. Chem. Fund 6 (1967) 527-539.
8. M. Syamlal, W. Rogers, T.J. O'Brien, MFIX Documentation: Theory guide, U.S. department of Energy (DOE), Morgantown Energy Technology Center, Morgantown, West Virginia, 1993.
9. S. Benyahia, M. Syamlal, T.J. O'Brien, Summary of MFIX equations 2005-4, 2007.
10. S. Benyahia, M. Syamlal, T.J. O'Brien, Extension of Hill-Koch-Ladd drag correlation over all ranges of Reynolds number and solids volume fraction. Powder Tech. 162 (2006) 166-174.
11. A. P. Baskakov, V. G. Tuponogov, N. F. Filippovski. A study of pressure fluctuations in a bubbling fluidized bed. Powder Tech. 45 (1986) 113-117.